Deuteron Relaxation Dispersion in Aqueous Colloidal Silica

Patrice Roose,*,† Henri Bauwin,‡ and Bertil Halle§

Physics Department, Vrije Universiteit Brussel, Pleinlaan 2, B-1050 Brussels, Belgium; Specialty Chemicals Division, DuPont Belgium, A. Spinoystraat 6, B-2800 Mechelen, Belgium; and Condensed Matter Magnetic Resonance Group, Department of Chemistry, Lund University, P.O. Box 124, S-22100 Lund, Sweden

Received: October 30, 1998; In Final Form: March 9, 1999

The magnetic relaxation dispersion from the water deuteron resonance in aqueous colloidal silica sols has been measured with the field-cycling technique in the frequency range from 1.5 kHz to 7.7 MHz. Dispersion profiles were recorded as a function of pL, L stands for a general hydrogen atom, in the range 2−11 for two sols with different particle size and at two temperatures. The profiles were well described by a Lorentzian dispersion function with an amplitude of β and an apparent correlation time of τ. The near invariance of τ with particle size, temperature, and pL demonstrates that the usual motional narrowing theory of spin relaxation is not applicable. A more general, nonperturbative theory, however, can quantitatively rationalize the data and yields, through a global fit, physically meaningful values of the microscopic parameters in the model. The analysis shows that the dispersion is partly due to long-lived water molecules and partly to silanol deuterons in rapid exchange with water. The silanol contribution is about 50% at pL 5, increasing to 90% at pL 8−10. Over most of the pL range, τ is essentially a measure of the residual quadrupole frequency of water and silanol deuterons and, hence, is not directly related to a motion in the system. The long-lived water molecules contributing to the dispersion have a residence time distribution spanning the microsecond range and are presumably trapped in micropores at the silica surface. The surface density of such trapped water molecules is found to be higher for silica particles of the more porous Stöber variety. The relaxation data also yield the surface density and orientational order parameter of silanol deuterons, as well as the rate constants for acid- and base-catalyzed silanol hydrogen exchange.

Introduction

Aqueous colloidal silica sols are used in diverse industrial applications, such as coatings, binders, microelectronics, and separation processes.[1,2] Suspensions of spherical particles of submicron size are also of fundamental interest as colloidal or macromolecular model systems. Many aspects of the morphology, molecular structure, and chemical activity of the silica surface have been elucidated by laser light scattering, electron microscopy, mass spectrometry, infrared and high-resolution NMR spectroscopy,[2−4] while information about the dynamic state of water at the surface of silica particles, porous glasses, and clays has come mainly from neutron scattering[5] and water ^{1}H, ^{2}H, and ^{17}O NMR relaxation.[6−13] If measured over a wide range of magnetic field strength and, hence, Larmor frequency, NMR relaxation times can provide direct information about interfacial water dynamics. In the case of silica sols, where there are motional components on the microsecond time scale, such relaxation dispersion studies must extend down into the kilohertz frequency range, accessible only with field-cycling techniques.[14] Previous contributions from this laboratory have reported and analyzed the longitudinal relaxation dispersion in the range 10^4−10^7 Hz of water protons in monodisperse colloidal silica suspensions prepared according to the Stöber method.[11−13] It was found that the relaxation dispersion comprises contributions from protons in long-lived water molecules as well as in silanol groups. Furthermore, the dispersion frequency was related to the mean residence time and the residual dipolar frequency of these protons.[13]

The magnetic relaxation of protons in diamagnetic aqueous systems is due to magnetic dipole−dipole interactions with nearby protons and is complicated by intermolecular interactions and cross-relaxation effects.[15] In contrast, the predominant relaxation mechanism of deuterons (spin $I = 1$) is the time modulation of the essentially intramolecular electric quadrupole interaction.[15] Since ^{2}H relaxation is not significantly affected by intermolecular magnetic interactions, it is much simpler to interpret. We have therefore conducted a ^{2}H field-cycling relaxation dispersion study of commercial (Syton, DuPont) and laboratory-prepared aqueous ($D_2O/H_2O \approx 9$) silica sols, reported herein. By pH-controlled variation of the acid- and base-catalyzed exchange rate of silanol deuterons, we could separate the contributions to the ^{2}H relaxation dispersion from rapidly exchanging silanol deuterons and long-lived water molecules. The apparent correlation time derived from Lorentzian fits to the relaxation dispersion profiles was found to be nearly independent of particle size and temperature and showed only a weak dependence on pH. This behavior is characteristic of the slow-motion regime, where the deuteron or water exchange rate does not exceed the quadrupole frequency, a fundamental assumption in the conventional perturbation theory of spin

* To whom correspondence should be addressed at UCB Chemicals, Anderlechtstraat 33, 1620 Drogenbos, Belgium. Tel: (32)-2-334 57 54. Fax: (32)-2-334 57 65. E-mail: Patrice.ROOSE@ucb-group.com.

† Vrije Universiteit Brussel.

‡ DuPont Belgium.

§ Lund University.

10.1021/jp984277l CCC: $18.00
Published on Web 06/09/1999

relaxation in liquids.[15] Using a more general, nonperturbative theory of spin relaxation of exchanging quadrupolar nuclei in locally anisotropic systems,[16] we can quantitatively account for the pH dependence of the dispersion amplitude and apparent correlation time. This analysis shows that the silanol contribution to the relaxation dispersion is substantial at all pH values and is dominant in the alkaline range. The pH-independent contribution from water deuterons is attributed to water molecules trapped in micropores at the silica surface and with a residence time distribution spanning the microsecond range. The ^{2}H relaxation dispersion behavior in silica sols is thus analogous to that in rotationally immobilized protein gels, where labile protein deuterons and long-lived water molecules trapped in internal cavities are responsible for the relaxation dispersion.[17]

Theoretical Background

Under the conditions of the present study, the longitudinal relaxation rate, R_1, of the observed water ^{2}H resonance can be expressed as a population-weighted average of the (apparent) local relaxation rates of bulk water deuterons (R_{bulk}), hydration water deuterons (R_W) and labile silanol deuterons (R_L) that exchange with the water deuterons[16−20]

$$R_1(\omega_0) = (1 - f_W - f_L)R_{bulk} + f_W\langle R_W(\omega_0)\rangle + f_L\langle R_L(\omega_0)\rangle \quad (1)$$

where f_X is the fractional population of deuterons in environment X (= W or L). The bulk solvent relaxation rate R_{bulk} was measured directly on a pure water reference sample of the same isotopic composition as the solvent in the silica sols. While eq 1 is valid only in the dilute regime ($f_X \ll 1$), it is not restricted to the fast-exchange regime. Deviations from the fast-exchange limit are implicitly accounted for in the apparent relaxation rates R_W and R_L (vide infra).

The dispersive contributions can be further subdivided on the basis of the time scales of the motions responsible for spin relaxation.[19] The investigated frequency range from 1 kHz to 10 MHz corresponds to motional correlation times from 10 ns to 0.1 ms. Faster motions, such as restricted rotation of silanol groups and long-lived hydration waters and the subnanosecond exchange and reorientation of the vast majority of hydration waters, make a frequency-independent contribution to R_1 but do not contribute to the observed dispersion. On the basis of previous ^{2}H and ^{17}O relaxation dispersion studies of protein solutions,[19−21] we expect that the dispersion from the silica sols is due to "internal" water molecules, trapped in micropores on the surface of the silica particles, and to labile deuterons residing in the surface silanol groups. As compared to typical protein solutions, however, the dispersion from the silica sols is displaced to lower frequencies by 2 orders of magnitude. This is due to the much larger size of the silica particles.

When, as is the case here, the Brownian rotation of the silica particles is slow compared to the residual quadrupole frequency Ω_Q ($1/\Omega_Q$ is on order 1 μs), then spin relaxation is induced by exchange of long-lived water molecules and silanol deuterons with bulk water and the relevant correlation time is the mean residence time of a deuteron in these sites. Unless all deuterons exchange rapidly compared to Ω_Q, the conventional perturbation theory of spin relaxation [15] breaks down and a nonperturbative approach much be used instead. For spin−1 nuclei such as ^{2}H and for dilute systems (f_W, $f_L \ll 1$, as is the case here), the generalized theory yields the following for the hydration water contribution in eq 1[16]

$$f_W R_W(\omega_0) = f_{WS}R_{WS} + f_{WI}\left\{R_{WI}^{loc} + \frac{2}{3}\Omega_{WI}{}^2 \times \left[\frac{0.2\tau_{WI}}{1 + (\Omega_{WI}\tau_{WI})^2 + (\omega_0\tau_{WI})^2} + \frac{0.8\tau_{WI}}{1 + (\Omega_{WI}\tau_{WI})^2 + (2\omega_0\tau_{WI})^2}\right]\right\} \quad (2)$$

which can be rewritten in the form

$$f_W R_W(\omega_0) = f_{WS}R_{WS} + f_{WI}\left\{R_{WI}^{loc} + \frac{2}{3}\frac{\Omega_{WI}{}^2}{\sqrt{1 + (\Omega_{WI}\tau_{WI})^2}}\left[\frac{0.2\tau'_{WI}}{1 + (\omega_0\tau'_{WI})^2} + \frac{0.8\tau'_{WI}}{1 + (2\omega_0\tau'_{WI})^2}\right]\right\} \quad (3)$$

where the apparent correlation time τ'_{WI} is given by

$$\tau'_{WI} = \frac{\tau_{WI}}{\sqrt{1 + (\Omega_{WI}\tau_{WI})^2}} \quad (4)$$

with τ_{WI} being the mean residence time of a trapped water molecule. Equation 4 shows that if $\tau_{WI} \gg 1/\Omega_{WI}$, the apparent correlation time deduced from eq 3 is nothing but the inverse of the residual quadrupole frequency Ω_{WI}. In the motional narrowing regime, where $\tau_{WI} \ll 1/\Omega_{WI}$, τ'_{WI} reflects the actual mean residence time. The residual quadrupole frequency is

$$\Omega_{WI} = \frac{3}{2}\pi S_{WI}\chi_{WI} \quad (5)$$

where S_{WI} is the orientational order parameter [22] of the water O−D bond and χ_{WI} is the ^{2}H quadrupole coupling constant in D_2O, for which we use the value of hexagonal ice (ice *Ih*), i.e., 213 kHz.[23] (The asymmetry parameter can be neglected.) The first term in eq 3 is the contribution from short-lived surface water molecules and the second term is due to local motions of long-lived trapped water molecules. We expect that $f_{WI} \ll f_{WS}$.

In analogy with eq 3, we have for the labile silanol deuterons:

$$R_L(\omega_0) = R_L^{loc} + \frac{2}{3}\frac{\Omega_L{}^2}{\sqrt{1 + (\Omega_L\tau_L)^2}}\left[\frac{0.2\tau'_L}{1 + (\omega_0\tau'_L)^2} + \frac{0.8\tau'_L}{1 + (2\omega_0\tau'_L)^2}\right] \quad (6)$$

where τ'_L and Ω_L are defined analogously to τ'_{WI} and Ω_{WI} in eqs 4 and 5. For χ_L we use the value 200 kHz.[19] The exchange of silanol deuterons in isotopic hydrogen mixtures is assumed to be catalyzed by L_3O^+ and OL^- ions according to[24]

$$\frac{1}{\tau_L} = k_1[L_3O^+] + k_2[OL^-] \quad (7)$$

where L stands for a general hydrogen atom. The prototropic ion concentrations were calculated as $[L_3O^+] = 10^{-pL}$ and $[OL^-] = 10^{pL-pK_W}$. For the dissociation constant of water (90.5/9.5% D_2O/H_2O at 7 °C) we used the value $pK_W = 15.46$, obtained by interpolation of the literature data.[25,26] The angular brackets in eq 1 denote averages over all sites of a given type (trapped water or silanol). This is primarily an average over the distribution of residence times (τ_{WI} or τ_L), reflecting the nonuniform morphology of the silica particle surface.

Materials and Methods

Sample Preparation. Two types of aqueous colloidal silica sols were studied. A commercially available silica sol, Syton

TABLE 1: Sol Characteristics

preparation	C (mg/mL)	d_{PCS} (nm)	τ_R (μs)[a]	A_{BET} (m^2/g)	A_{Sears} (m^2/g)
S1	127 ± 1	17	1.2	222 ± 1	
SW50	733 ± 2	54	38	63.5 ± 0.1	77

[a] Calculated from d_{PCS} with solvent viscosity for 90%/10% D_2O/H_2O at 7 °C.

W50 (Lot 5C202), was kindly provided by DuPont-Belgium. The silica particles in this sol were produced by an inorganic synthesis process known as the ion-exchange method, which usually yields particles of low surface porosity but relatively high size polydispersity.[1] In the following, this preparation is referred to as SW50. The second silica sol, referred to as S1, was prepared in this laboratory according to the method of Stöber et al.[27] The silica particles are formed through hydrolysis and condensation of tetraethoxysilane, TES = $Si(OC_2H_5)_4$, in a mixture of water, ammonia, and ethanol. In general, Stöber silica particles are quite porous[28] but fairly monodisperse as compared to the commercial SW50 particles. The S1 preparation was also used in a previous relaxation dispersion study,[13] to which we refer for details of the preparation.

Prior to $H_2O \rightarrow D_2O$ exchange, pH was adjusted by addition of small amounts of HCl or NaOH to an aliquot of the stock suspension. The deuterated samples were prepared by addition of D_2O (Aldrich, 99.96 atom % ^2H, low in paramagnetic impurities) to a 90:10 volume ratio. The solvent deuteron fraction x in the NMR samples (i.e. the ratio of deuteron isotopes to the total number of hydrogen atoms in the solvent) was typically 0.905 (S1) or 0.925 (SW50). The pH* value, measured with a conventional pH meter equipped with a combined Ag−AgCl/glass electrode and a saturated KCl salt bridge after calibration in standard H_2O buffers, was converted to a generalized pL scale according to[29]

$$pL = pH^* + 0.3314x + 0.0766x^2 \quad (8)$$

The pH* value was checked after the NMR relaxation measurements. The estimated pH* error is 0.1, and the variation upon deuteration did not exceed 0.2 units.

Sol Characterization. The characteristics of the stock suspensions are reported in Table 1. The translational diffusion coefficient of the particles in the sols was determined by photon correlation spectroscopy (PCS). The PCS data were analyzed with the multiexponential fitting package CONTIN, which is based on the optimization of an extended least-squares estimation problem.[30] The effect of interparticle interactions on the measured diffusion coefficient was assessed from a set of measurements at different silica concentrations, and the single-particle diffusion coefficient was obtained by linear extrapolation to infinite dilution. Finally, the hydrodynamic diameter, d_{PCS}, and the rotational correlation time, τ_R, of the particles was estimated from the Stokes−Einstein relation.[30]

The particles were also characterized by nitrogen adsorption measurements performed on a Coulter SA 3100 surface analyzer. According to the BET procedure, the specific surface area, A_{BET}, of the dried silica material can be estimated from the adsorption isotherm data within the relative pressure range 0.05−0.3.[31] Since the measured surface area is limited by the occupied area of the adsorbate gas molecules (16.2 $Å^2$ for N_2), it may not exactly reflect the accessibility of water molecules to the rough particle surface. A comparison of the BET surface area with the area obtained from hydroxide ion titration by the method of Sears[1] provides an indication of the microporosity of the surface. The specific surface area A_{Sears} in Table 1 was supplied by the manufacturer for the sample SW50 and suggests that even this preparation has a significant microporosity.

The silica mass fraction was determined gravimetrically by heating 5 mL of the stock suspension in an oven at 120 °C for 24 h. The electrolyte content in the dry residue was neglected. Mass fractions were converted to silica concentrations, expressed in units of mass per volume, using the values 2.0 and 2.2 g cm^{-3} for the density of Stöber[32] and commercial[1] silica, respectively.

Relaxation Measurements. The magnetic field dependence of the deuteron longitudinal relaxation time T_1 in the range from 0.23 mT to 1.2 T was measured at the Vrije Universiteit Brussel using an electronically switched 7.5 MHz field-cycling relaxation spectrometer, designed following ideas developed for the IBM relaxometer by Koenig and Brown.[33] A description of the field-cycling principle and the technical specifications of the instrument can be found elsewhere.[11,12] Each magnetization signal was measured three times in order to improve the signal-to-noise ratio. The longitudinal relaxation time was obtained from a monoexponential fit to the decay of the average magnetizations as a function of evolution delay. Some of the measurements were repeated several times, and the final profiles are reported as weighted averages. The deuteron relaxation dispersion curves were measured at 7 and 20 °C. The temperature was regulated by a preheated stream of nitrogen gas and checked just before and after the measurements using a thermocouple immersed in a dummy water sample. The uncertainty of the temperature was ±0.5 °C. Independent measurements of the solvent deuteron relaxation rate in a 90% D_2O/10% H_2O mixture yielded R_{bulk} = 3.99(± 0.04) s^{-1} and 2.59(± 0.02) s^{-1} at 7 and 20 °C, respectively. As expected, R_{bulk} was independent of magnetic field.

In contrast to the laboratory-prepared Stöber silica, commercial silica sols commonly contain trace amounts of paramagnetic contaminants that cannot easily be removed.[11,12] At alkaline pH values, paramagnetic metal ions (e.g. Mn^{2+}, Fe^{3+}, Cu^{2+} ions) are adsorbed on the colloidal surface. From a former study of the paramagnetic relaxation effects in colloidal silica, it has been shown that adsorbed ions gives rise to a substantial proton relaxation enhancement at high magnetic fields (0.25−1.2 T) where the colloidal silica barely contribute to the proton relaxation enhancement.[12] The proton relaxation enhancement in this field range provides thus a suitable control of the extent of the paramagnetic effects and was found to be very low for the commercial SW50 sample. Taking the lower gyromagnetic ratio of the deuterons and the solvent dilution into account, one can reasonably assume that the paramagnetic relaxation effects are unimportant for the deuteron relaxation. This was experimentally corroborated by addition of Mn^{2+} ions to the deuterated colloidal silica samples, in amounts causing a significant enhancement of the proton relaxation rates. No increase of the deuteron relaxation rates could be evidenced in this case (unpublished results).

Results and Discussion

Qualitative Features. Figures 1 and 2 show water ^2H relaxation dispersions from the colloidal silica preparation S1 at two pL values at 7 °C and for the SW50 preparation at 7 and 20 °C. In Figure 1, the relaxation rate R_{bulk} of the pure solvent (90/10% D_2O/H_2O) is also indicated. The magnetic field strength is expressed as the ^2H Larmor frequency, $\nu_0 = \omega_0/2\pi$. The relatively large scatter in the data, as compared to corresponding ^1H data,[13] is essentially due to the lower signal-to-noise ratio of the ^2H magnetization signal. The silica particles produce a

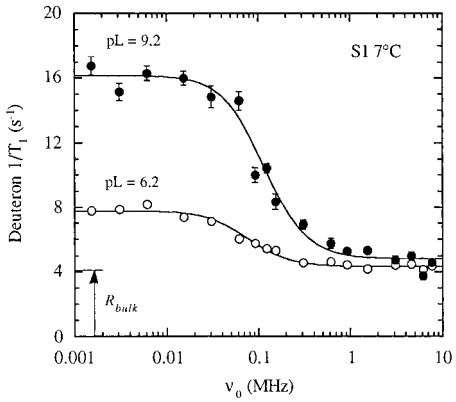

Figure 1. Deuteron relaxation dispersion of the Stöber silica sample S1 (12.2 mg/mL, 7 °C) at the pL values 6.2 and 9.2. The bulk solvent relaxation rate, R_{bulk}, is also indicated. The curves resulted from nonlinear least-squares fits of the three parameters α, β, and τ in eq 9.

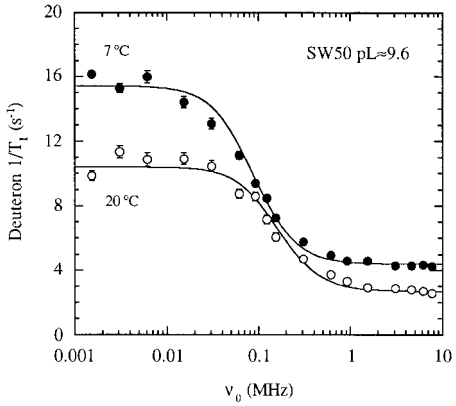

Figure 2. Deuteron relaxation dispersion of the silica sample SW50 at pL 9.6 and temperatures 7 °C (66.7 mg/mL) and 20 °C (61.1 mg/mL). The curves resulted from nonlinear least-squares fits of the three parameters α, β, and τ in eq 9.

solvent relaxation enhancement over the entire investigated frequency range from 1.5 kHz to 7.7 MHz and the enhancement is more pronounced at alkaline pL values. The curves in Figures 1 and 2 resulted from weighted nonlinear least-squares fits to the expression[20]

$$R_1(\omega_0) = \alpha + \beta\left[\frac{0.2\tau}{1+(\omega_0\tau)^2} + \frac{0.8\tau}{1+(2\omega_0\tau)^2}\right] \qquad (9)$$

The standard deviations in the three adjustable parameters α, β, and τ were estimated according to the theory of the minimum variance bound.[34] The ^{2}H dispersion profiles are fairly well represented by this Lorentzian dispersion function. In contrast, the ^{1}H relaxation dispersion in diamagnetic silica sols is not adequately described by eq 9.[13] This difference reflects the fact that the ^{2}H quadrupole coupling is intramolecular, with a similar value in water and in silanol groups, whereas the ^{1}H dipole−dipole coupling is partly intermolecular, with a consequent spread of dipole coupling strengths.

To separate the relaxation contributions from trapped water molecules and labile silanol deuterons, relaxation dispersions were recorded over a wide pL range. At each pL value, the parameters α, β, and τ were determined from fits to eq 9. Figures 3*a*,*b* show the pL dependence of the high-frequency relaxation excess, $\tilde{\alpha} \equiv \alpha - R_{bulk}$, and the dispersion amplitude factor β for the preparations S1 and SW50 at 7 °C. The parameter values are scaled to a silica concentration of 10 mg mL^{-1} to compensate for concentration differences between the samples. For preparation S1, the pL dependencies of $\tilde{\alpha}$ and β are qualitatively similar. The large relaxation enhancement at alkaline pL is attributed to base-catalyzed exchange of labile silanol deuterons. For preparation SW50, a similar behavior is found for the β factor but not for $\tilde{\alpha}$, which is independent of pL within the experimental uncertainty. The reduction of β for SW50 as compared to S1 is partly due to the smaller specific surface area of the SW50 particles. However, the ratio of the β factors for the two preparations, which is 5−6 over the entire pL range, exceeds the ratio of the BET specific surface areas, ca. 3.5 (Table 1). This discrepancy suggests that N_2 adsorption does not quantitatively reflect the effects of microporosity on silanol group exposure and the prevalence of water-accessible micropores. (The specific surface area obtained from water vapor or OH^- adsorption would have been more appropriate for comparing with the dispersion amplitude β, but unfortunately, it was not available for the S1 preparation.) Figure 3c shows that β is nearly independent of temperature over the entire pL range.

Figure 4 shows the pL dependence of the apparent correlation time τ for preparations S1 and SW50 at 7 °C and for preparation SW50 at 7 and 20 °C. With values between 0.5 and 2.5 μs, the variation of τ is remarkably small. The near invariance of τ with particle size and temperature demonstrates that the relaxation dispersion is not governed by the rotational diffusion of the silica particles. If this were the case, we would expect a 50% increase of τ on going from 20 to 7 °C (due to increased solvent viscosity) and a 30-fold increase of τ on going from S1 to SW50 particles (since the rotational correlation time should scale as d_{PCS}^3). The water ^{2}H relaxation dispersion behavior observed here for silica particles contrasts with that seen in solutions of small- and medium-sized proteins,[19−21] where τ can usually be identified with the rotational correlation time (τ_R) of the protein (on the order of 10 ns). This qualitative difference is due to the several orders of magnitude longer τ_R is for the much larger silica particles (Table 1). It might then be expected that τ should be governed by the exchange of trapped water molecules and labile silanol deuterons with bulk water according to[20] $\tau = (1/\tau_R + 1/\tau_X)^{-1} \approx \tau_X$ (X = WI or L). However, also this hypothesis can be refuted by the results in Figure 4, since the residence time τ_X should depend strongly on temperature (for trapped water and silanol deuterons) and on pL (for silanol deuterons; see eq 7).

A ^{2}H relaxation dispersion centered around 0.1 MHz, corresponding to an apparent correlation time of ca. 1 μs, signals the breakdown of the motional narrowing theory.[16,17] Using a more general, nonperturbative approach, it can be shown [16,17] that if $\tau_R > 1/\Omega_Q$, where Ω_Q is the residual quadrupole frequency in eq 5, and if there is a distribution of residence times τ_X covering a range around $1/\Omega_Q$, then the relaxation rate will be dominated by residence times near $1/\Omega_Q$ and the dispersion will occur at a frequency corresponding to a correlation time $\tau \approx 1/\Omega_Q$ (see eq 4). As long as we are in this slow-motion regime, the apparent correlation time τ will be independent of system variables such as temperature, pL, and particle size. Under these conditions, τ is essentially a nuclear property and cannot be associated with the time scale of any molecular motion in the system. The order of magnitude of the apparent correlation time τ determined here (Figure 4) as well as its near invariance with respect to particle size, temperature, and pL clearly demonstrates that slow-motion effects are important for ^{2}H relaxation in aqueous silica sols.

Quantitative Interpretation. A quantitative analysis of the dispersion parameters α, β, and τ must be based on the generalized relaxation theory. By comparing the fitting function

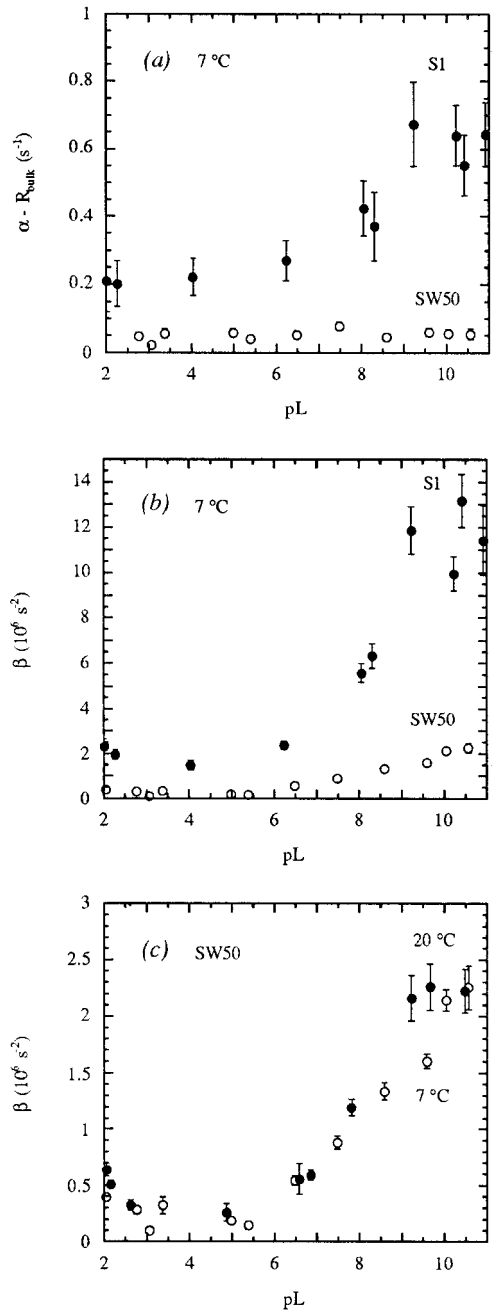

Figure 3. Variation with pL of (a) the high-frequency excess relaxation rate $\alpha - R_{bulk}$ and (b) the dispersion amplitude factor β for the silica preparations S1 and SW50 at 7 °C. The pL dependence of β for preparation SW50 at 7 and 20 °C is shown in (c). The parameters were scaled to a silica concentration of 10 mg/mL.

in eq 9 with the microscopic expressions in eqs 1 − 6, the parameters α, β, and τ can be related to the molecular properties of the system. Before discussing the dispersion, described by β and τ, we briefly consider the high-frequency relaxation parameter α.

For the high-frequency relaxation enhancement, we obtain

$$\tilde{\alpha} \equiv \alpha - R_{bulk} = f_{WS}(\langle R_{WS}\rangle - R_{bulk}) + f_{WI}(\langle R_{WI}^{loc}\rangle - R_{bulk}) + f_{L}(\langle R_{L}^{loc}\rangle - R_{bulk}) \quad (10)$$

Since restricted rotational motions (librations) of trapped water molecules and of silanol groups are expected to occur on a picosecond time scale and since f_{WI} and $f_L \ll f_{WS}$, we neglect the second and third terms in eq 10. (The symmetric 180° flip

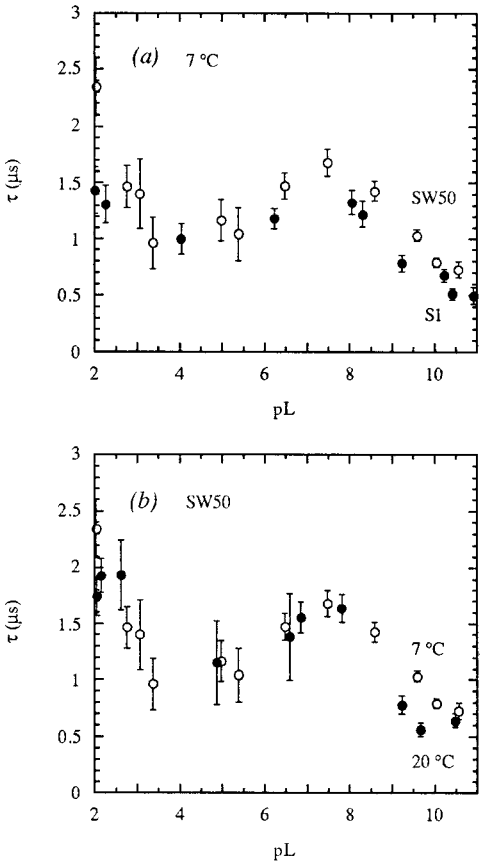

Figure 4. Variation with pL of the apparent correlation time τ for silica preparations S1 and SW50 at 7 °C (a) and for preparation SW50 at 7 and 20 °C (b).

of a trapped water molecule can be much slower,[35] but this motion has no effect on the water ^{17}O relaxation rate[20] which, after normalization by R_{bulk}, is similar to the ^2H rate for silica sols in the megahertz frequency range[7]). It is known that the surface-induced perturbation of the rate of water reorientation is short-ranged, being essentially confined to water molecules in direct contact with the surface.[6] We thus estimate f_{WS} for a monolayer of water (0.15 nm^2 $molecule^{-1}$) on a smooth spherical silica particle of diameter d_{PCS} (Table 1). From the $\tilde{\alpha}$ values in Figure 3*a*, we can then calculate the ratio $\langle R_{WS}\rangle/R_{bulk}$, which can be interpreted as the ratio $\langle \tau_{WS}\rangle/\tau_{bulk}$ of rotational correlation times of surface and bulk water. We thus obtain $\langle \tau_{WS}\rangle/\tau_{bulk}$ values between 140 (low pL) and 460 (high pL) for the S1 preparation and an average value of 130 for the SW50 preparation. These values are much higher than the dynamic retardation factor $\langle \tau_{WS}\rangle/\tau_{bulk} = 5.4$ obtained for a monolayer of water on the surface of sodium hectorite clay sheets[6] and the similar values obtained for the surface hydration of globular proteins,[19−21] phospholipid,[36] and surfactant[37] interfaces. This discrepancy might indicate a population of water molecules with residence times in the range 1−10 ns. These putative water molecules should reside in surface pockets and crevices that are less exposed than the micropores occupied by the fraction f_{WI} of very long-lived water molecules (see below). They would give rise to a dispersion in the range 10−100 MHz, i.e., above the frequency window examined here. A previous water ^2H and ^{17}O relaxation study of silica sols did indeed find a significant frequency dependence in the range 4−50 MHz.[7] In that study, the silica concentration was more than an order of magnitude higher than here. At the lower concentration used here, the difference $R_1 - R_{bulk}$ at the highest frequencies is not much larger than the experimental error (Figure 1), so the $\tilde{\alpha}$ contribu-

tion cannot be accurately determined. Indeed, the pL dependence of $\tilde{\alpha}$ for preparation S1 may be a fitting artifact due to an increasing deviation from Lorentzian dispersion shape at higher pL. (This would have little effect on the much larger β contribution.)

To analyze the pL dependence of the dispersion parameters β and τ, we calculated the dispersive part, $R_1 - \alpha$, of the relaxation rate at 20 logarithmically spaced frequencies ν_0 in the range from 1 kHz to 10 MHz and performed a nonlinear least-squares fit to the dispersive part of the fitting function in eq 9. According to eqs 1−6,

$$R_1 - \alpha = \left\langle \beta_{WI}\left[\frac{0.2\tau'_{WI}}{1+(\omega_0\tau'_{WI})^2} + \frac{0.8\tau'_{WI}}{1+(2\omega_0\tau'_{WI})^2}\right]\right\rangle + \left\langle \beta_L\left[\frac{0.2\tau'_L}{1+(\omega_0\tau'_L)^2} + \frac{0.8\tau'_L}{1+(2\omega_0\tau'_L)^2}\right]\right\rangle \quad (11)$$

where the angular brackets denote averages over the distributions of the residence times τ_{WI} and τ_L, and

$$\beta_{WI} = \frac{2}{3} f_{WI} \frac{\Omega_{WI}^2}{\sqrt{1+(\Omega_{WI}\tau_{WI})^2}} \quad (12)$$

with an analogous relation for β_L. Furthermore, the effective correlation time τ'_{WI} and the residual quadrupole frequency Ω_{WI} are given by eqs 4 and 5, respectively, with analogous relations for τ'_L and Ω_L. The quadrupole coupling constants χ_{WI} and χ_L were assigned values of 213 and 200 kHz, respectively (see above), and τ_L was computed from eq 7. The rotational diffusion of the silica particles was taken into account by replacing τ_L by $1/(1/\tau_L + 1/\tau_R)$.[20] Finally, the fractional populations f_{WI} and f_L , which are in the range $10^{-6} - 10^{-4}$, were calculated from

$$f_{WI} = \frac{6\phi\nu_W\sigma_{WI}}{(1-\phi)d} \quad (13)$$

$$f_L = \frac{3\phi\nu_W\sigma_L}{(1-\phi)d} \quad (14)$$

where $\nu_W = 0.030$ nm^3 is the molecular volume of bulk water, d the silica particle diameter (Table 1), and ϕ the silica particle volume fraction, obtained by dividing the silica concentration (10 mg mL^{-1} after normalization) by the mass density of the silica particles (see above). Finally, σ_{WI} and σ_L are the surface densities of trapped water molecules and silanol groups, respectively.

Since β and τ do not depend much on temperature (Figures 3c and 4b), we focus on the 7 °C data for the two preparations. For a given set of the eight microscopic parameters, τ_R, τ_{WI}, σ_{WI}, σ_L, S_{WI}, S_L, k_1, and k_2, we used the protocol described above to calculate β and τ as functions of pL. All parameters were taken to be independent of pL. This was the case also for σ_L, although it is known that about 20% of the silanol groups are deprotonated at pH 10.[28,38] The microscopic parameters were then varied to bring the theoretical curves into agreement with the experimentally derived β and τ data in Figures 3c and 4b. The agreement improved substantially by invoking a distribution of k_2 values, taken to be uniform on a logarithmic scale and extending over two decades centered on the reported k_2 value. Physically, this distribution reflects the heterogeneous surface morphology, giving rise to variable solvent exposure of silanol groups. For the same reason, a similar distribution was invoked for the trapped-water residence time τ_{WI}. This had a much smaller effect, however. Finally, the full protocol was implemented as a global nonlinear least-squares fit of the microscopic parameters to the combined β and τ data. The resulting fits are shown in Figure 5 and the parameter estimates are collected in Table 2. The quantitative agreement with experimental, evident in Figure 5, suggests that our theoretical description of water ^{2}H relaxation dispersion in silica sols contains the essential ingredients.

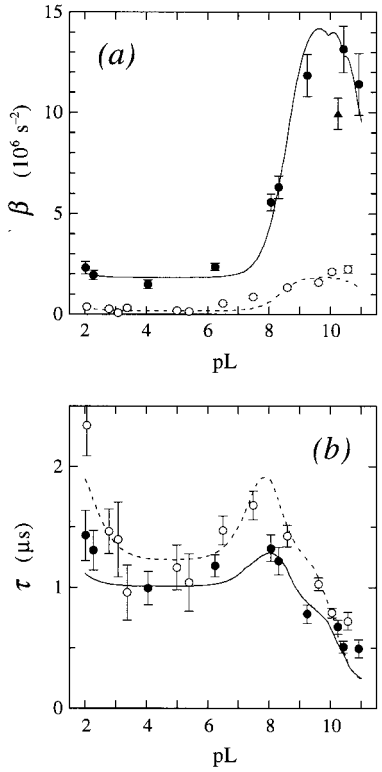

Figure 5. Variation with pL of the dispersion amplitude factor β and the apparent correlation time τ for silica preparations S1 (solid symbols and curves) and SW50 (open symbols, dashed curves), both at 7 °C. The curves resulted from nonlinear least-squares fits to the combined β and τ data for each preparation, with the parameter values in Table 2. The outlying β value at pL 10.24 was not included in the fit (triangle, S1 series).

TABLE 2: Parameter Values Derived from Fits to pL Dependence of β and τ

parameter	S1	SW50
τ_R (μs)	60 ± 25	140 ± 50
τ_{WI} (μs)	2[a,b]	2[a,b]
k_1 (10^6 M^{-1} s^{-1})	0.8 ± 0.7[b]	3.0 ± 0.7[b]
k_2 (10^{12} M^{-1} s^{-1})	1.0 ± 0.1[b]	1.0 ± 0.1[b]
σ_{WI} (nm^{-2})	0.10 ± 0.02	0.04 ± 0.01
σ_L (nm^{-2})	3.1 ± 0.4	3.0 ± 0.2
S_{WI}^2	0.9[a]	0.9[a]
S_L^2	0.48 ± 0.06	0.23 ± 0.02

[a] Parameter value frozen during fit. [b] Logarithmically uniform distribution spanning two decades and centered on the quoted value.

The pL dependence of β and τ can now be rationalized. In the theory, pL enters solely via the silanol deuteron residence time τ_L in eq 7. With the rate constants k_1 and k_2 according to Table 2, τ_L has a maximum of 30 ms at pL 4.7 (S1) or 15 ms at pL 5.0 (SW50). In the pL range 3−7, we have $\tau_L > \tau_R$, so $\tau'_L \rightarrow 1/\Omega_L = 1.52$ μs (S1) or 2.22 μs (SW50), and the factor $[1+(\Omega_L\tau_L)^2]^{-1/2} \rightarrow 1/(\Omega_L\tau_R)$, which governs β (see eq 12), is also nearly constant. This is illustrated in Figure 6. At pL 7−8, there is a crossover and at still higher pL values $\tau_L < \tau_R$ so that τ'_L and $[1+(\Omega_L\tau_L)^2]^{-1/2}$ become controlled by the strongly

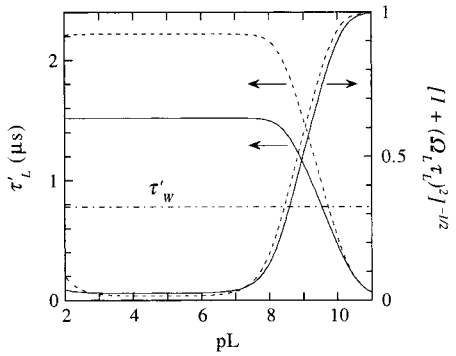

Figure 6. Variation with pL of the renormalized silanol deuteron residence time τ'_L (left) and the renormalization factor $[1 + (\Omega_L\tau_L)^2]^{-1/2}$ (right). The curves were calculated with the parameter values in Table 2 for preparations S1 (solid curves) and SW50 (dashed curves).

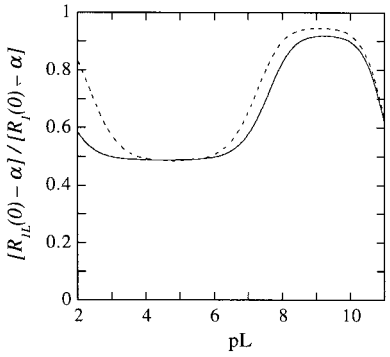

Figure 7. Relative contribution to the ^{2}H relaxation dispersion step from silanol deuterons as a function of pL. The curves were calculated with the parameter values in Table 2 for preparations S1 (solid curves) and SW50 (dashed curves).

pL-dependent silanol exchange time τ_L. At pL 10, $\tau_L = 0.3$ μs and $(\Omega_L\tau_L)^2 \ll 1$ so that we enter the motional narrowing regime, where $\tau'_L \approx \tau_L$ and the factor $[1 + (\Omega_L\tau_L)^2]^{-1/2}$ approaches unity (Figure 6). A similar behavior occurs at low pL (<3) due to acid-catalyzed silanol exchange, but this range is barely probed by the data. The pL dependence of β in Figure 5a is essentially a reflection of the factor $[1 + (\Omega_L\tau_L)^2]^{-1/2}$ in the silanol contribution to the dispersion step (cf. Figures 5a and 6). According to the fit, the slight decrease of β above pL 10 is due to the reduction of τ_L, which decreases the relative silanol contribution to the dispersion step (Figure 7) and, hence, gives more weight in the Lorentzian fit to the trapped-water contribution with $\beta_{WI} < \beta_L$ (since $\sigma_{WI} \ll \sigma_L$). The neglected deprotonation of silanol groups (decrease of σ_L), however, might also contribute to the observed reduction of β.

According to eq 4 and the parameter values in Table 2, $\tau'_{WI} = 0.93$ μs, independent of pL. Due to the assumed distribution of τ_{WI}, however, $\langle\tau'_{WI}\rangle = 0.78$ μs. Below pL 8, τ_L, $\tau_R \gg 1/\Omega_L$, so $\tau'_L = 1/\Omega_L = 1.52$ μs (S1) or 2.22 μs (SW50). The apparent correlation time τ derived from the fit to the Lorentzian dispersion function in eq 9 is essentially a weighted average of τ'_{WI} and τ'_L. Since the relative weight of the silanol contribution increases below and above pL 5 (Figure 7) and since $\tau'_L > \tau'_{WI}$, it follows that τ exhibits a minimum around pL 5 (Figure 5b). The decrease of τ above pL 8 results from the shortening of τ'_L by base catalysis as τ_L becomes comparable to and then shorter than $1/\Omega_L$ (Figures 5b and 6).

We now consider the parameter values in Table 2. Since the trapped-water contribution to the relaxation dispersion does not depend on pL, it is not possible to separately determine the three parameters τ_{WI}, σ_{WI}, and S_{WI} from the observed pL dependence of β and τ. In the fits, we have therefore frozen two of these parameters to the values $\tau_{WI} = 2$ μs and $S_{WI}^2 = 0.9$. We thus assume that the water molecules trapped in silica micropores are highly ordered, like water molecules buried in small protein cavities,[39] and that they have a logaritmically uniform residence time distribution in the range $0.2 < \tau_{WI} < 20$ μs. Nearly indistinguishable curves can be generated for other combinations of values for these frozen parameters, with little effect on the silanol-related parameters. A trapped-water residence time distribution spanning the microsecond range is required, however, to account for the experimental results. It should also be noted that, since water molecules with residence times much shorter or much longer than $1/\Omega_{WI}$ contribute little to the dispersion (see Figure 1 in ref 17), the actual density of trapped water molecules can be higher than the value σ_{WI} corresponding to the postulated logarithmic distribution over two decades. Conversely, if the τ_{WI} distribution happened to be peaked near 1 μs, the density would be lower. Nevertheless, the finding that the trapped-water density σ_{WI} is significantly higher for the S1 particles than for the SW50 particles (Table 2) is consistent with the more pronounced microporosity of the former (cf. Materials and Methods).

More definite information is obtained about the silanol-related parameters. The values 3.0 and 3.1 nm^{-2} obtained for σ_L are lower than the value 5 nm^{-2} for a fully hydroxylated silica surface,[1-3] as expected, since we have neglected deprotonation of silanol groups at high pL. The mean-square silanol O−D bond order parameter, $S_L^2 = 0.48$ (S1) or 0.23 (SW50), represents the effect of partial orientational averaging by submicrosecond motions, including rotation around the Si−O bond. The acidic rate constant, $k_1 = (0.8-3.0) \times 10^6$ M^{-1} s^{-1} is on the same order of magnitude as found for hydroxyl groups in proteins.[40] The basic rate constant, $k_2 = 1 \times 10^{12}$ M^{-1} s^{-1}, however, is higher than expected even for a diffusion-controlled process. This could indicate either that hydroxide ions accumulate near the silica surface (despite its negative net charge) or that the kinetics is not properly described by eq 7. The silanol hydrogen exchange rate constants, in particular k_2, are accurately determined even from unconstrained fits (no frozen parameters). A reduction of k_2 would shift the pL maxima in β and τ to higher pL. Finally, we note that the derived values for the silica particle rotational correlation time, $\tau_R = 60$ μs (S1) and 140 μs (SW50), are considerably larger than those predicted by the PCS particle diameters (Table 1), although the variation with particle size is in the right direction. This apparent discrepancy may be related to the fact that the theory used here is based on a strong-collision model, where the correlation time refers to a jumplike process that completely randomizes the orientation.[16] This model is appropriate for hydrogen exchange from silanol groups to bulk water, but not for rotational diffusion of the silica particles. The rotational correlation time τ_R is the time taken for the second-rank orientational correlation function to decay to 37% ($1/e$) of its initial value. In our ad hoc extension of the strong-collision theory, featuring an effective correlation time $1/(1/\tau_L + 1/\tau_R)$, one should therefore use a value for τ_R that is longer than the actual rotational correlation time. This conclusion is supported by the observation that τ differs little between the S1 and SW50 particles (Figure 5b), although $\tau_R \approx 1$ μs for the smaller S1 particles according to the PCS results.

Conclusions

Using the field-cycling technique, we have measured the ^{2}H relaxation dispersion from aqueous silica sols for the first time. The most striking aspect of the results is the near invariance of

the apparent correlation time τ with particle size, temperature, and pL, showing that it cannot be directly identified with a molecular motion in the system. To account for these observations, it is necessary to invoke a nonperturbative relaxation theory valid for arbitrarily slow motions, i.e., under conditions where the conventional motional-narrowing theory of spin relaxation fails. In the motional narrowing limit, $(\Omega_Q\tau_X)^2 \ll 1 + (\omega_0\tau_X)^2$, motions with frequencies matching the Zeeman level spacing (ω_0) are most efficient in inducing (longitudinal) relaxation. In the opposite limit, motions with frequencies matching the pure quadrupole level spacing (Ω_Q) are most efficient. In the silica sols studied here, both the water and silanol relaxation contributions exhibit strong slow-motion effects, and the pL variation of τ reflects the changing relative weights of these contributions as the silanol exchange rate varies. In the commonly studied pL range 8−10, the relaxation dispersion is strongly dominated (>90%) by exchanging silanol deuterons. This should also be the case for the transverse relaxation rate R_2 at all frequencies, as previously concluded[7] on the basis of high-frequency ^{2}H and ^{17}O relaxation measurements (although the arguments were partly based on the inadequate motional narrowing theory). For the sols investigated here, the silanol contribution to the dispersion step is substantial (ca. 50%) even at pL 5, where the silanol exchange rate is minimal. Under these conditions, the silanol contribution is limited by the rotational diffusion of the silica particles, which is in the slow-motion limit, where $R_{1L}(0) - \alpha \propto 1/\tau_R$. The silanol contribution should therefore be less important for larger particles.

The simultaneous analysis of the pL variation of the dispersion amplitude β and the apparent correlation time τ provides quantitative information about the microdynamics at the silica/water interface. The resulting silanol group density, $\sigma_L = 3$ nm^{-2}, is compatible with independent estimates. The mean-square order parameter, S_L^2, for the silanol O−D bond is in the range 0.23−0.48 depending on silica preparation. If this is ascribed entirely to rotation around the Si−O bond, it corresponds to a Si−O−D angle of 144−153°. The rate constant, $k_2 = 1 \times 10^{12}$ M^{-1} s^{-1}, of base-catalyzed silanol deuteron exchange is 1−2 orders of magnitude higher than expected, suggesting a local accumulation of hydroxide ions at the interface or a deviation from second-order kinetics. The contribution of water to the relaxation dispersion can be accounted for by a relatively low density ($\sigma_{WI} = 0.1$ nm^{-2}, corresponding to about 90 water molecules per S1 particle) of highly ordered ($S_{WI}^2 = 0.9$) water molecules, or by a larger number of less ordered water molecules. In any case, the residence time distribution must span the microsecond range. Most likely, these long-lived water molecules occupy micropores at the silica surface. Furthermore, a population of water molecules with residence times in the range 1−10 ns is indicated by the high-frequency relaxation data, in addition to the vast majority of kinetically labile (ps range) exposed water molecules at the silica surface.

In previous work,[11−13] the relative independence of the proton relaxation dispersion upon variation of particle size, pH, and temperature was also observed. This suggests an interpretation similar to the one described here for the deuteron relaxation dispersion. However, the heterogeneity of proton environments at the silica surface causes a substantial broadening of the proton relaxation dispersion profile, which impedes a straightforward quantitative analysis to confirm this hypothesis.

Acknowledgment. We are grateful to Prof. R. Finsy of the Vrije Universiteit Brussel for his assistance in sample characterization, Ig. C. De Greef and O. Devroede for their help in the relaxation dispersion measurements, and Prof. J. Van Craen for the many interesting discussions.

References and Notes

(1) Iler, R. K. *The Chemistry of Silica*; Wiley: New York, 1979.
(2) Bergna, H. E. In *The Colloid Chemistry of Silica*; Bergna, H. E., Ed.; American Chemical Society: Washington, DC, 1994; pp 1−47.
(3) Zhuravlev, L. T. *Colloids Surf.* **1993**, *74*, 71.
(4) Maciel, G. E. In *Nuclear Magnetic Resonance in Modern Technology*; Maciel, G. E., ed.; NATO ASI series, Kluwer: Dordrecht, 1994; p 401.
(5) Ramsay, J. D. F.; Poinsignon, C. *Langmuir* **1987**, *3*, 320.
(6) Woessner, D. E. *J. Magn. Reson.* **1980**, *39*, 297.
(7) Picullel, L. *J. Chem. Soc., Faraday. Trans. 1* **1986**, *82*, 387.
(8) Gillis, P.; Borcard, B. *J. Magn. Reson.* **1988**, *77*, 19.
(9) Stapf, S.; Kimmich, R.; Niess, J. *J. Appl. Phys.* **1994**, *75*, 529.
(10) Stapf, S.; Kimmich, R. *J. Chem. Phys.* **1995**, *103*, 2247.
(11) Roose, P.; Van Craen, J.; Finsy, R.; Eisendrath, H. *J. Magn. Reson. A* **1995**, *115*, 20.
(12) Roose, P. Ph.D. Thesis; Vrije Universiteit Brussel, 1997.
(13) Roose, P.; Van Craen, J.; Eisendrath, H. *Colloids Surf. A*, **1998**, *145*, 213.
(14) Noack, F. *Prog. NMR Spectrosc.* **1986**, *18*, 171.
(15) Abragam, A. *Principles of Nuclear Magnetism*; Clarendon Press: Oxford, 1961.
(16) Halle, B. *Prog. NMR. Spectrosc.* **1996**, *28*, 137.
(17) Halle, B.; Denisov, V. P. *Biophys. J.* **1995**, *69*, 242.
(18) Zimmerman, J. R.; Brittin, W. E. *J. Phys. Chem.* **1957**, *61*, 1328.
(19) Denisov, V. P.; Halle, B. *J. Mol. Biol.* **1995**, *245*, 698.
(20) Halle, B.; Denisov, V. P.; Venu, K. In *Modern Techniques in Protein NMR*; Berliner L. J., Krishna, N. R. Eds.; Plenum: New York, 1998; Vol. 17.
(21) Denisov, V. P.; Halle, B. *Faraday Discuss.* **1996**, *103*, 227.
(22) Halle, B.; Wennerström, H. *J. Chem. Phys.* **1981**, *75*, 1928.
(23) Edmonds, D. T.; Mackay, A. L. *J. Magn. Reson.* **1975**, *20*, 515.
(24) Eigen, M. *Angew. Chemie (Int. Ed.)* **1964**, *3*, 1.
(25) Gold, V. *Adv. Phys. Org. Chem.* **1969**, *7*, 259.
(26) Covington, A. K.; Robinson, R. A.; Bates, R. G. *J. Phys. Chem.* **1966**, *70*, 3820.
(27) Stöber, W.; Fink, A.; Bohn, E. *J. Colloid Interface Sci.* **1968**, *26*, 62.
(28) de Keizer, A. *Proceedings of the 10th ECIC*; Turku, Finland, 1996.
(29) Salomaa, P.; Schaleger, L. L.; Long, F. A. *J. Am. Chem. Soc.* **1964**, *86*, 1.
(30) Finsy, R. *Adv. Colloid Interface Sci.* **1994**, *52*, 79.
(31) Brunauer, S.; Emmett, P. H.; Teller, E. *J. Am. Chem. Soc.* **1938**, *60*, 309.
(32) van Blaaderen, A.; Kentgens, A. P. M. *J. Non-Cryst. Solids* **1992**, *149*, 161.
(33) Koenig, S. H.; Brown III, R. D. *Prog. NMR Spectrosc.* **1991**, *22*, 487.
(34) Sorenson, H. W. *Parameter Estimation: Principles and Problems*; Marcel Dekker: New York, 1980.
(35) Larsson, K.; Tegenfeldt, J.; Hermansson, K. *J. Chem. Soc., Faraday Trans.* **1991**, *87*, 1193.
(36) Volke, F.; Eisenblätter, S.; Galle, J.; Klose, G. *Chem. Phys. Lipids* **1994**, *70*, 121.
(37) Carlström, G.; Halle, B. *Langmuir* **1988**, *4*, 1346.
(38) Bolt, G. H. *J. Phys. Chem.* **1957**, *61*, 1166.
(39) Denisov, V. P.; Venu, K.; Peters, J.; Hörlein, H. D.; Halle, B. *J. Phys. Chem. B* **1997**, *101*, 9380.
(40) Liepinsh, E.; Otting, G.; Wüthrich, K. *J. Biomol. NMR* **1992**, *2*, 447.